This article has been accepted for publication in a future issue of this journal, but has not been fully edited. Content may change prior to final publication. Citation information: DOI 10.1109/TNSRE.2017.2771273, IEEE Transactions on Neural Systems and Rehabilitation Engineering

Improved prosthetic control based on myoelectric pattern recognition via wavelet-based de-noising

Julian Maier, Adam Naber, and Max Ortiz-Catalan, *Member, IEEE*

***Abstract*—Real-time inference of human motor volition has great potential for the intuitive control of robotic devices. Towards this end, myoelectric pattern recognition (MPR) has shown promise in the control of prosthetic limbs. Interfering noise and susceptibility to motion artifacts have hindered the use of MPR outside controlled environments, and thus represent an obstacle for clinical use. Advanced signal processing techniques have been previously proposed to improve the robustness of MPR systems. However, the investigation of such techniques have been limited to offline implementations with long time windows, which makes real-time use unattainable. In this work, we present a novel algorithm using discrete and stationary wavelet transforms for MPR that can be executed in real-time. Our wavelet-based de-noising algorithm outperformed conventional band-pass filtering (up to 100 Hz) and improved real-time MPR in the presence of motion artifacts, as measured by the Motion Test. Improved signal-to-noise ratio was found not to be crucial in offline MPR, as machine learning algorithms can integrate high but consistent noise as part of the signal. However, varying interference is expected to occur in real life where signal processing algorithms, as the one introduced in this study, would potentially have a positive impact. Further implementation of these algorithms in a prosthetic embedded system is required to validate their feasibility and usability during activities of the daily living.**

***Index Terms*—Artificial neural networks (ANN), prosthetic limbs, myoelectric pattern recognition, discrete wavelet transforms, signal denoising.**

I. Introduction

Restoring the pre-amputation functional state after limb loss using artificial devices is a challenging task. In recent decades, improvements in fields pertaining to prosthetic technology have been reported [1]. Commercially available prosthetic hardware combined with digital state-of-the-art technology has the potential to profoundly improve the functionality of limb prostheses. Electromyography (EMG) could hereby provide an intuitive human-machine interface for prosthetic control.

State-of-the-art prostheses utilize a couple of EMG sites and finite-state machines to control many functions [2]. The serial manner of this type of prosthetic control is counterintuitive and does not allow simultaneous actuation of multiple degrees of freedom (DoF). Limb prostheses under this control scheme are far from resembling the functionality of their biological counterpart.

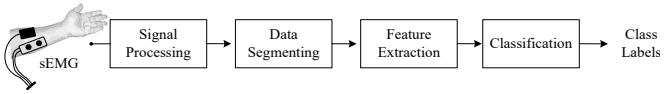

Fig. 1. Main processing stages in MPR for myoelectric control.

Myoelectric prostheses use and abandonment is affected by a wide range of factors such as comfort, durability, function, control, and appearance. Surveys report higher rejection rates for electric devices compared to body-powered prostheses [3]. Poor controllability is believed to be a major reason for the low acceptance rate of myoelectric prostheses among upper-limb amputees [4].

Myoelectric pattern recognition (MPR) has shown promising results over the last decades as a solution for dexterous multifunction prosthetic control. Approaches in pattern recognition commonly include fundamental processing stages, which are depicted in Fig. 2. However, the enthusiasm emerging within the academic community is met by poor clinical and commercial impact [4, 1]. Currently there is only one commercially available MPR system from which clinical results are to be reported (Coapt, USA).

The MPR approach for prosthetic control has several shortcomings that could explain why its acceptance is lower than the high classification accuracies obtained in laboratory evaluations would suggest. A critical challenge is to maintain long-term stability and robustness in the decoding of motor volition, for which a clean and consistent EMG signal seems to be a prerequisite.

During surface EMG signal acquisition, various physiological and external background noise sources and artifacts interfere, *e.g.* electrode shifts or liftoff, movement related artifacts, physiological noise, or external mechanical interferences. Most of the noise sources can be mitigated under

Manuscript received December 14, 2016. This work was supported by the Promobilia foundation, and VINNOVA.

J. Maier is at the Institute of Signal Processing and System Theory, University Stuttgart, Germany (e-mail: julian.maier@mail.com)

A. Naber is at the Department of Electrical Engineering, Chalmers University of Technology (e-mail: naber@student.chalmers.se).

M. Ortiz-Catalan is at the Department of Electrical Engineering, Chalmers University of Technology, and Integrum AB, Sweden (e-mail: maxo@chalmers.se).

This article has been accepted for publication in a future issue of this journal, but has not been fully edited. Content may change prior to final publication. Citation information: DOI 10.1109/TNSRE.2017.2771273, IEEE Transactions on Neural Systems and Rehabilitation Engineering

relatively static laboratory conditions. However, in real-life operation, the execution of motion and its muscle contractions are performed under a wide variety of dynamic conditions within which noise or artifacts are unavoidable — conceivably making the signal unrecognizable for a classifier.

Previous research on MPR has been mainly focused on feature extraction, classification, and post-processing strategies. Signal pre-processing techniques, which have a direct impact on MPR accuracy, have been scarcely investigated despite indications of potential improvements by using algorithms such as wavelet de-noising [5, 6, 7]. To our best knowledge, no scientific investigation dealing with stationary wavelet transform-based de-noising in real-time of EMG signals for MPR has been published. Most of the previous work on similar algorithms is not suitable for real-time processing due the use of long time windows [8] or high sampling rates [9]. None of the recently proposed approaches in signal pre-processing such as class-wise principle component analysis [10], independent component analysis [11], signal whitening [12], advanced autoregressive processing [13], or wiener filtering [14, 15] have been evaluated in real-time, which is a requirement for further clinical translation.

In the present study, we employed discrete and stationary wavelet transform-based de-noising techniques to improve the quality of the EMG signals prior to real-time MPR for the control of upper-limb prostheses. This approach was motivated by the ability of wavelet-based de-noising as a shape-conserving, noise filtering technique [7].

Firstly, we systematically evaluated the capability of wavelet-based de-noising to reduce unavoidable random background noise, which cannot be removed by conventional band-pass filtering. Secondly, we present a novel algorithm to mitigate the impact of motion artifacts and mechanical disturbances on MPR accuracy. High-pass filtering at 10 Hz or 20 Hz has been proposed as the most immediate solution, due to the electric characteristics of motion related artifacts (mainly located in the lower frequencies) [16]. However, we found that conventional high-pass filtering with cutoff frequency as high as 100 Hz, is not reasonably effective against strong motion related artifacts and extrinsic mechanical disturbances (*i.e.,* rapid limb movements), arguably because these eminently overlap the EMG frequency spectrum.

All signal processing algorithms in this work were subject to the constraint of real-time computation to guarantee their usability in MPR-based prosthetic systems. This posed the challenges of maximizing functionality and performance, while keeping the complexity and the response time at a minimum. Furthermore, the classification ability must not deteriorate from signal treatment when favorable acquisition conditions are present. Here we showed that wavelet-based de-noising can be performed within real-time constraints, and it does not decrease system performance under favorable conditions.

This study was approved by the Regional Ethics Committee in Gothenburg, Sweden.

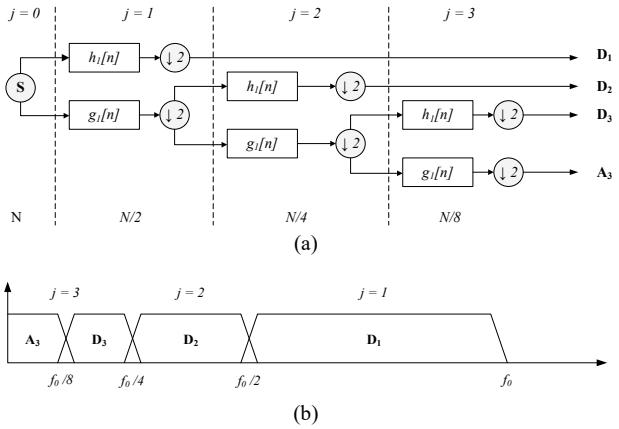

Fig. 2 (a) DWT filter bank scheme of a third-level DWT decomposition. The original signal (S) passes a series of complementary high- and low-pass filters ($h_1[n]$ and $g_1[n]$, respectively) which coefficients are calculated from a chosen wavelet function $\psi(t)$ and its corresponding scaling function $\phi(t)$. The signal (S) emerges as two signals: Approximation (A) and detail coefficients (D), which are subsequently down-sampled by a factor of two. The decomposition is repeated, using the A array as an input for the following filters. This procedure is repeated until the desired level of depth J, resulting in the final approximation (A_J) and all level details (D_1-D_J). (b) Coefficient arrays and corresponding frequency sub-bands with f_0. equal to the Nyquist frequency.

II. Background

A. Wavelet transform

The wavelet transform (WT) decomposes a signal from the time-domain into multi-resolution components, called the time-frequency representation. WT has been growing in popularity in EMG analysis as it enables a high time-resolution at ascending frequencies combined with high frequency-resolution in the lower frequency components. WT can be categorized into discrete and continuous forms. The discrete wavelet transform (DWT) is most commonly used in EMG analysis, as the processing time is low and its implementation conveniently employs the fast wavelet transform (FWT) by using filter banks (see Fig. 2a) [17]. The DWT of an input signal $x(t)$ and a given discrete wavelet $\psi_{j,k}$ can be written as:

$$C_{j,k} = \sum_{t\in\mathbb{Z}} x(t)\,\psi_{j,k}(t) \quad \text{with} \quad \psi_{j,k} = \frac{1}{\sqrt{2^{-j}}}\psi(2^j t - k),$$

where $C_{j,k}$ are the wavelet coefficients with a discrete mother wavelet ψ dyadic scaled by 2^{-j} and translated by $k \cdot 2^{-j}$ with $j \in \mathbb{N}$ and $k \in \mathbb{Z}$. WT can hence be seen as a projection onto a set of child wavelets $\psi_{j,k}$ which form an orthonormal system in the space of $L^2(\mathbb{R})$. The original signal $x(t)$ is hereby decomposed into wavelet coefficients of each level j, which corresponds to denoted frequency bands (see Fig. 2b). The resulting wavelet coefficients are true components of the original signal $x(t)$ without any loss of data, which allows for a perfect reconstruction, namely the Inverse Discrete Wavelet Transform (IDWT).

This article has been accepted for publication in a future issue of this journal, but has not been fully edited. Content may change prior to final publication. Citation information: DOI 10.1109/TNSRE.2017.2771273, IEEE Transactions on Neural Systems and Rehabilitation Engineering

B. Stationary wavelet transform (SWT)

Critical sub-sampling makes DWT the most efficiently computed wavelet transform. However, DWT suffers from variance to time shifts. This might be without consequence due to the perfect reconstruction ability of inverse DWT, but it becomes critical when translation-invariant signal analysis is performed in the wavelet coefficient subspace.

SWT achieves translation-invariance by using a redundant wavelet representation as the signal sub-sampling in the DWT is removed (see Fig. 3). Instead, the filter coefficients are up-sampled by a factor of 2^j in the *j*-th level of the algorithm. The basic idea is to average slightly different DWT, so called ε-decimated DWT (for a rigorous proof, refer to [18]).

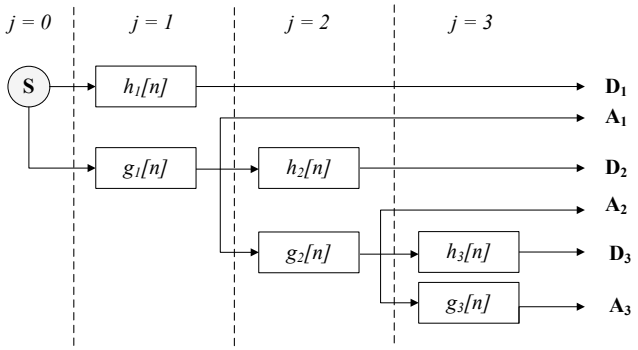

Fig. 3 SWT Filter bank scheme of a third-level DWT decomposition.

C. Wavelet-based de-noising

The objective of wavelet-based de-noising is to recover the signal of interest from a noisy composition. In MPR, the task concerns finding coefficients in the wavelet transformed subspace that contain deterministic, distinguishable information. In wavelet-based de-noising, undesired corrupted coefficients resulting from random noise can be modified prior to the reconstruction process to produce a cleaner signal. This approach involves three main steps (see Fig. 5): (1) Wavelet decomposition using DWT or SWT of specified level *J*; (2) Coefficient thresholding based on level-wise noise level estimation; and (3) Reconstruction of the signal via inverse DWT/SWT from the modified coefficients. To achieve and optimize the de-noising procedure, several points need to be addressed, such as selection of a suitable wavelet function, type, and depth of the decomposition, noise level estimation, and coefficient thresholding (see Table 1).

Table 1 Wavelet de-noising parameters used for evaluation.

Wavelet transform	DWT, SWT, SWT + WCF
Wavelet level depth	3,4, and 5
Noise level estimation (level-dependent)	universal, GSMU, SURE, minimax, penalized
Coefficient thresholding	hard, soft, adaptive, improved, hyperbolic, non-negative Garrote
Wavelet basis functions	db1, db2, db3, db4, sym2, sym3, sym4 coif1, coif2, coif3 bior1.3, bior1.5, bior2.2, bior2.4, rbio1,3, rbio1.5, rbio2.2, rbio2.4

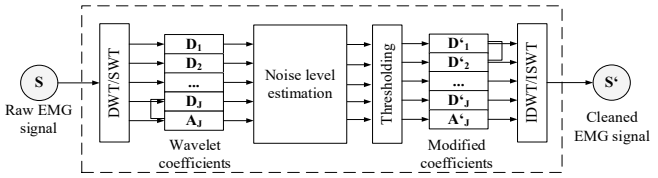

Fig. 5 Basic wavelet de-noising scheme.

D. Wavelet Wiener filtering

Wiener filtering needs an *a priori* estimate of the desired noise-free signal for calibration. Wiener filtering assumes the signal and the artifact to be stationary, linear, stochastic processes with known spectral characteristics. A linear time invariant Fourier filter is therefore used in the frequency domain, where the original Fourier coefficients are rescaled according to the ratio between the desired and actual signal spectrum. Wiener filtering can also be applied in the wavelet domain, namely wavelet Wiener filtering (WWF) [19], which is illustrated in Fig. 4. Employment of the Wiener correction factor has been explored for ECG signal filtering [20], but no available literature was found discussing wavelet Wiener filtering for EMG signal processing.

WWF hereby defines the Wiener Correction Factor (WCF) $\hat{g}_m(n)$ as:

$$\hat{g}_m(n) = \frac{\hat{u}_m^2(n)}{\hat{u}_m^2(n)+\hat{\sigma}_m^2(n)},$$

where $\hat{u}_m$ equals the squared wavelet coefficients obtained from the estimate $s(n)$ and $\hat{\sigma}_m(n)$ is the variance of the noise coefficients in the *j*-th decomposition level. The modified wavelet coefficients ${}^{\lambda}y_m(n)$ are finally obtained by:

$${}^{\lambda}y_m(n) = y_m(n) \cdot \hat{g}_m(n)$$

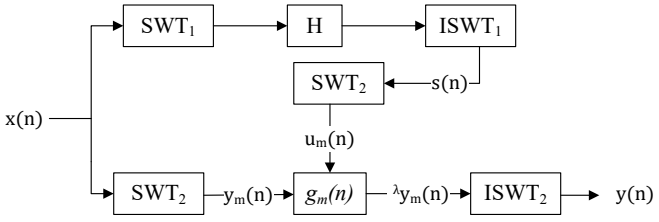

Fig. 4 Basic scheme of the wavelet Wiener filtering approach.

III. METHODOLOGY

A. Wiener correction factor

Sharing the same wavelet function and level depth among the first (SWT_1) and second wavelet decomposition (SWT_2) provides the opportunity to calculate the WCF $\hat{g}_m(n)$ by a single wavelet decomposition. For the purpose of wavelet de-noising, we implemented WWF in this simplified form to enhance computational speed, which is crucial for real-time execution. We investigated the performance of Wiener corrected SWT-based de-noising with bior1.3 wavelets, adaptive thresholding, and minimax threshold selection.

This article has been accepted for publication in a future issue of this journal, but has not been fully edited. Content may change prior to final publication. Citation information: DOI 10.1109/TNSRE.2017.2771273, IEEE Transactions on Neural Systems and Rehabilitation Engineering

B. Real-time artifact reduction algorithm

Our wavelet-based approach follows three main steps to detect and reduce interfering artifacts:

1) *Wavelet decomposition* using a fourth level SWT with Daubechies 1 wavelets to minimize processing time. The time-frequency representation is used for the temporal detection of artifacts. SWT was preferred owing to its time-invariant nature.

2) *Thresholding*: We sampled EMG signals at 2000 Hz. The approximation level hereby corresponds to a frequency range between 0–62.5 Hz. The sub-band of the third detail coefficients represents frequencies in the range of 125–250 Hz, and therefore contains the dominant frequency components of the myoelectric signal. Artifact-free EMG data should be represented by high values of the third detail coefficients and lower valued approximation coefficients, which motivated our definition of an artifact detection threshold θ as:

$$\theta_k = \text{median}(|D_3|) + k \cdot \sigma(D_3),$$

where D_3 are all detailed coefficients in the third level, σ is the standard deviation of these coefficients, and k is a parameter which allows level dependent threshold adjustment. All approximation coefficients exceeding θ are considered to be compromised by an artifact. Hard thresholding is subsequently applied:

$$A_s = \begin{cases} 0, & \text{if } A_s > \theta_1 \\ A_s, & \text{otherwise} \end{cases},$$

where $s \in [1, N]$ denotes the location of the coefficients within the time window of sample length N. Since artifacts can contain frequency components higher than the frequencies that are represented by the approximation coefficients of our used fourth level decomposition, thresholding has consequently been extended to the detail coefficients at the n-th level $D_{n,s}$:

$$D_{n,s} = \begin{cases} 0, & \text{if } D_{n,s} > \theta_0 \vee A_s > \theta_1 \\ D_{n,s}, & \text{otherwise} \end{cases},$$

where $n = 1,2,3$ and 4 and k was set to zero.

3) *Signal reconstruction* of the modified coefficients.

C. Signal acquisition, processing, classification

A set of surface EMG recording from 10 non-amputee subjects performing 10 hand and wrist motions was used for offline evaluation of wavelet de-noising, as well as for assessing the performance of the artifact reduction algorithm here proposed. This data set of myoelectric signals is provided in the *BioPatRec* open source platform under the label "10mov8ch-Untargeted-Forearm" [21]. The EMG signals were recorded from four bipolar electrodes (Ag/AgCl, 1 cm diameter, and 2 cm inter-electrode distance) equally spaced around the most proximal third of the forearm, and sampled at 2 kHz with 14-bits in resolution. Recordings were taken on the left arm and all subjects were right-handed, their average age was 33.9±13 years old, and 60% were males.

We evaluated the real-time performance of the motion reduction algorithm in six able-bodied subjects. Subjects used their left arm, five were right-handed, and five were males. Six motion classes were investigated (hand open/close, wrist flexion and extension, and forearm pronation and supination) by using four pairs of disposable electrodes in the same way as the offline evaluation. The subjects were visually guided by the *BioPatRec* recording graphical user interface [21]. Training sessions contained three repetitions of each motion, each lasting for 3 s and relaxing/resting periods of the same length between each contraction. The intensity of the contractions was requested to be around 70–80% of the maximum voluntary contraction, which was visually verified by the overall EMG magnitude during muscular contractions. Signals were sampled at 1 kHz with 24-bits in resolution using an in-house designed EMG acquisition system [22].

The raw EMG signals of each recorded motion were symmetrically trimmed to 70% of the contraction time and the time window size was set to 256 ms with a time increment of 64 ms. The four most commonly used time-domain features in MPR (Mean Absolute Value [MAV], Wave-Length [WL], Zero-Crossing [ZC], and Slope-Sign-Changes [SSC]) were extracted from the resulting time windows to form the feature vectors, which were then fed to the classifiers.

We employed a Linear Discriminant Analysis (LDA) classifier (MATLAB ® Statistics and Machine Learning Toolbox, Mathworks, Inc., USA) and a Multi-Layer Perceptron (MLP) classifier (NetLab Toolbox Version 3.3.1, [23]). The NetLab MLP uses logistic sigmoid activation functions for the hidden layer. The output layer uses a softmax function, which has shown the best results for single class activation. The maximum number of iterations in the learning procedure was set to 400.

All algorithms were implemented in the modular open source platform *BioPatRec* [24]. Segment-wise processing time of all algorithms was measured to assess their real-time feasibility. Offline and real-time data processing was performed in MATLAB 2015b (Mathworks, Inc., USA) using an i7-4500 CPU @1.8 GHz.

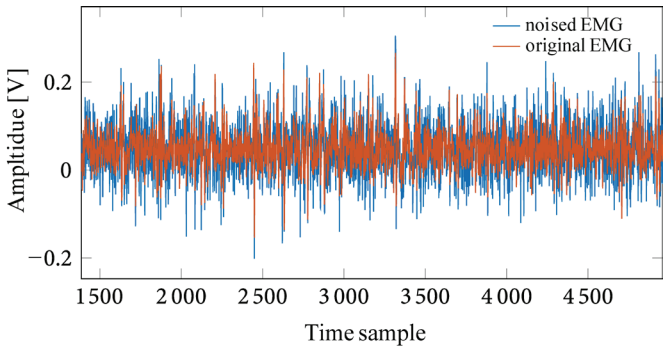

Fig. 6 Original EMG signal (red) and noisy version (blue), which was calculated by using uniformly distributed random numbers with zero mean and standard deviation (SD) of 10% of the largest SD, which was found during a single contraction of all EMG signals obtained for one subject. Using this approach, the signal power of the additive noise was equal throughout all movements and channels.

This article has been accepted for publication in a future issue of this journal, but has not been fully edited. Content may change prior to final publication. Citation information: DOI 10.1109/TNSRE.2017.2771273, IEEE Transactions on Neural Systems and Rehabilitation Engineering

D. Offline evaluation criteria

We chose Mean Squared Error (MSE), Signal-to-Noise Ratio (SNR), and classification accuracy (Acc) as performance criteria to evaluate the signal treatment regimes offline.

1) *MSE* was defined as:

$$\mathrm{MSE} = \sum_{i=1}^{N} \frac{\left(s_{\mathrm{noise,f}} - s_{\mathrm{raw,f}}\right)^2}{i},$$

where N is the total number of the analyzed overlapping time windows, s_{raw} represents the original acquired EMG signal samples while s_{noise} represents its artificially created noisy samples. The index f indicates that the samples have been filtered/modified. The larger the MSE, the greater the difference between the samples of the de-noised and the true signals.

2) MSE by itself was not considered sufficient to estimate the de-noising performance as it does not reflect the remaining information content of the signal after filtering has been applied. This motivates to define a *SNR* index:

$$\mathrm{SNR} = 10 \log\left(\frac{P_{s_{\mathrm{noise,f}}}}{P_{e_{\mathrm{noise}}}}\right) \mathrm{dB}.$$

The noise power $P_{e_{\mathrm{noise}}}$ is based on the noise estimation function $e_{\mathrm{noise}} = s_{\mathrm{noise,f}} - s_{\mathrm{raw,f}}$ which represents the remaining noise after signal de-noising or artifact reduction have been performed.

3) Classification accuracy was used to assess the de-noising performance for the classification task. *Acc* represents the averaged accuracy rates over all motions and all EMG data sets:

$$\mathrm{Acc} = \frac{\text{absolutely correct class predictions}}{\text{total class predictions}} \cdot 100\%,$$

Improved accuracy is defined as:

$$\mathrm{Acc}_{\mathrm{improved}} = \mathrm{Acc}_{\text{de-noised}} - \mathrm{Acc}_{\text{no de-noising}}.$$

Using wavelet de-noising as an estimation tool to generate an improved EMG signal in terms of both class separability and robustness, we desire small MSE values while having a high SNR. In order to find the best set of parameters for wavelet de-noising and to assess the performance of the artifact reduction algorithm, signals were compromised with either random noise (see Fig. 8) or insertion of previously recorded artifacts (see Fig. 11).

These were inserted into the untreated original EMG signals, which served as reference datasets in accordance to the following settings:

1) *Noise$_{AllSets}$*: Noise/artifacts were added throughout the reference EMG signals before window segmenting is applied and can therefore be found in all time windows.

2) *Noise$_{TestingSet}$*: Noise/artifacts are not present in the training set, but appear in the testing set to assess the performance of the classifier with unseen data. This means that untampered data was used during learning, as would normally be the case, while noise and artifacts appear during testing, resembling the operational situation. This method allowed us to systematically evaluate the robustness of the classification under changing noise levels or novel artifacts in real-time.

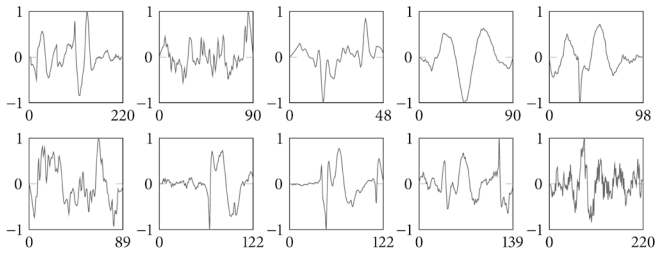

Fig. 7 Recorded artifacts of different length [ms], elicited by rapid limb movements, electrode tapping or cable movement. Amplitudes are normalized between -1 and 1. The Noise$_{\mathrm{AllSet}}$ contained artifacts with an average time gap of 1s throughout the entire EMG recordings, whereas the Noise$_{\mathrm{TestingSet}}$ setting contained artifacts with an average time gap of 200ms within the testing data set. Magnitudes of the inserted artifacts were randomly set within a range between one to tour times of the overall MAV of the trimmed EMG recording.

E. Wavelet de-noising parameter optimization

Firstly, the optimal wavelet decomposition level was selected. Phinyomark *et al.* investigated the level depth with different wavelet functions and found that the third and fourth levels at 2000 Hz sampling frequency, resulting in approximation coefficients at the 0-62.5 Hz and 0-31.25 Hz frequency bands respectively, are better than other levels. They also showed that the overall trend is not affected by the choice of the wavelet function [7]. Using subject-specific wavelet functions for de-noising has been investigated, but the results showed that more work on a generic wavelet tuned to sEMG needs to be performed to be useful in a real-life setting [25]. We found that fifth level decompositions perform similar compared to fourth level decompositions. Fourth level de-noising performed even better in regards of the defined SNR criterion; this holds true for both SWT and DWT de-noising. These results support that fourth level decompositions are sufficient, as no improvement of a fifth level decomposition was observed. As a result, fourth level decompositions were used for further evaluation.

Secondly, coefficient shrinking methods were evaluated for DWT- and SWT-based de-noising. In addition to the traditional and commonly used hard and soft coefficient shrinkage, four modified thresholding functions were evaluated. We found that adaptive shrinkage gave the best results for both DWT and SWT de-noising. The results are in accordance with the studies by Phinyomark *et al.* [7], which showed that adaptive is the best wavelet shrinkage method in both the de-noising and the pattern recognition points of view.

Selecting the optimal threshold value is another crucial part of wavelet de-noising. Therefore, six different threshold selection rules were evaluated.

Finally, wavelet basis functions with various orders from five different families were employed: Daubechies (db), Symlets (sym), Coiflets (coif), BiorSplines (bior) and ReverseBior (rbio). Error measures and accuracies from 18 wavelet functions were evaluated (see Table 1). The simplest wavelet db1 outperforms all other wavelets in both MSE and SNR. In

This article has been accepted for publication in a future issue of this journal, but has not been fully edited. Content may change prior to final publication. Citation information: DOI 10.1109/TNSRE.2017.2771273, IEEE Transactions on Neural Systems and Rehabilitation Engineering

case of prosthetic control, the short filter length of the db1 wavelet is additionally desirable, as it reduces computation time.

F. *Real-time evaluation with Motion Test*

The Motion Test was used to evaluate the wavelet based artifact reduction algorithm in a real-time environment. This test was originally introduced by Kuiken *et al.* [26] and was used in this study as implemented in BioPatRec [24]. As it is impractical to create an equal appearance of artifacts in different real-time sessions for a single subject, we individually collected the three different types of artifacts (see Fig. 7) and fused these during the motion test with the real-time EMG signal in a pseudo-random manner to mimic an unpredictable occurrence. This was done in order to ensure equivalent appearance of the artifacts during motion test trials. The individually extracted artifacts were continually introduced in randomly selected channels (1 up to 4) with an average time gap of 0.5 s and a randomly determined magnitude of up to 100 µV, which corresponded to 78–213% of the maximum amplitude of the subject's EMG signals.

This approach was necessary to obtain reliable results for a paired comparison between trials of the Motion Test. The subjects were requested to perform each motion class randomly by following instructions displayed by *BioPatRec*. Each subject performed two consecutive trials of the Motion Test in which each movement was performed three times with a time out of 10 seconds using MLP for classification.

Motion Tests were performed with conventional high-pass filtering of 20 Hz. The proposed wavelet artifact reduction algorithm was utilized in one of them to compared it with high-pass filtering only. We focused on two metrics of the Motion Test: completion time and real-time accuracy. Completion time is defined as the time from the first prediction other than rest to the 20th correct classification. The fastest possible completion time of any motion was 4 s, corresponding to 20 consecutive correct predictions with new predictions occurring every 200 ms. The median values for each motion (three repetitions) were selected for each participant and averaged across the six participants. Real-time accuracy is the percentage of correct predictions over the total number of predictions during the completion time. A paired t-test was used to evaluate statistically significant differences at $p < .05$.

IV. Results and Discussion

A. *Wavelet de-noising parameter optimization*

We found that simple wavelets with short filter length provide better results than wavelets of higher orders. Hence, it is advisable to use wavelets of a low order for wavelet de-noising. Accuracies by LDA and MLP classification provided corroborated this conclusion. Bior1.3 and bior1.5 performed best in the $\text{Noise}_{\text{TestingSet}}$ setting among all the wavelets employed, outperforming db1, which had shown the best error values. An evaluation of 53 wavelet functions by Phinyomark *et al.* [7] confirms the tendencies observed in the MSE and SNR results. Minimax and universal selection rules provided promising results in terms of MSE and SNR. We could see

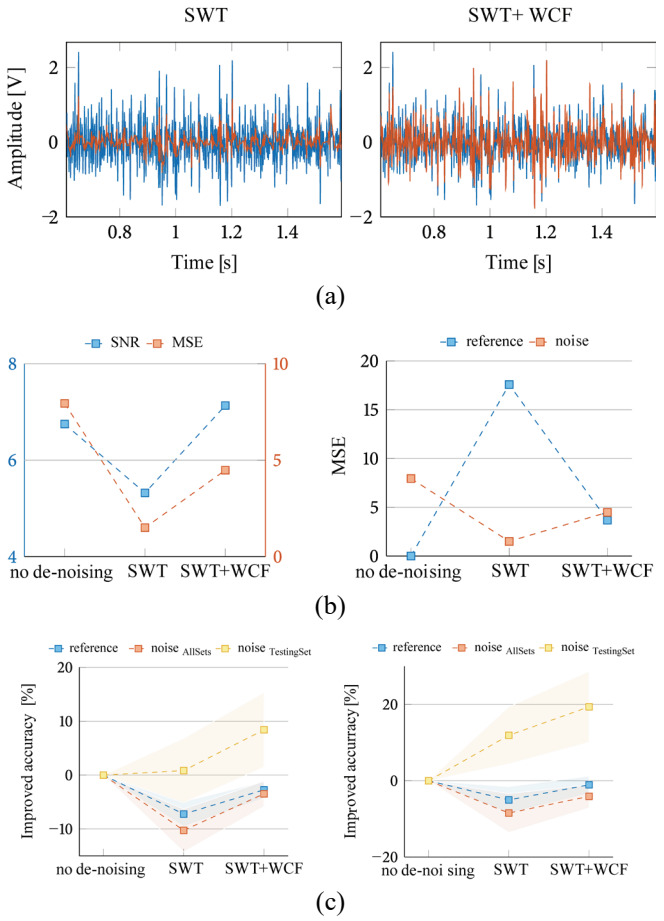

Fig. 8 (a) De-noised signals (red lines) of noisy EMG signals (blue lines) with (right) and without (left) application of Wiener correction factor (b) Error measures (c) Changes in classification accuracies with LDA (left) and MLP (right). Shaded error bars represent SD of the averaged EMG recording sessions (n=10).

different tendencies between the original EMG, the $\text{Noise}_{\text{AllSets}}$ and the $\text{Noise}_{\text{TestingSet}}$ setting. Moreover, the results based on MLP and LDA classification, respectively, vary widely from one another, which makes it difficult to give a recommendation for optimal de-noising performance.

B. *Usage of Wavelet wiener filtering*

Fig. 8a illustrates the EMG de-noised signals with and without usage of the WCF. It can be seen that the WCF recovers signal components which would have been discarded during classical wavelet thresholding. At the same time, using WCF yields a higher MSE value, but is accompanied by an increased SNR (see Fig. 8b). This observation raises the question of whether the retrieved signal components are beneficial in terms of class separability and robustness against changing noise. From Fig. 8c it is evident that using WCF in wavelet de-noising has positive effects on the classification performance. We can see an improvement throughout all settings investigated for both LDA and MLP classification.

C. *SWT- vs. DWT-based de-noising*

The experiments performed to find an optimal set of wavelet de-noising parameters showed analogous results for SWT- and DWT-based de-noising procedures regarding tendencies

This article has been accepted for publication in a future issue of this journal, but has not been fully edited. Content may change prior to final publication. Citation information: DOI 10.1109/TNSRE.2017.2771273, IEEE Transactions on Neural Systems and Rehabilitation Engineering

between the evaluated parameters. The performance of SWT and DWT was evaluated by using favorable parameters: bior1.3 wavelets, fourth level decomposition and level dependent adaptive thresholding combined with WCF. The resulting signal after SWT de-noising using the parameters mentioned is depicted in Fig. 9.

As it can be seen from Fig. 10a, SWT-based de-noising outperformed DWT-de-noising in terms of MSE and SNR. These results were confirmed by the calculated classification accuracies, particularly when MLP classification was performed (see Fig. 10b). Notwithstanding, Fig. 10b shows that in case of LDA classification, SWT de-noising leads to reduced classification performance in the reference and in the $\text{Noise}_{\text{AllSets}}$ condition and therefore cannot improve the accuracy under a high, consistent level of noise.

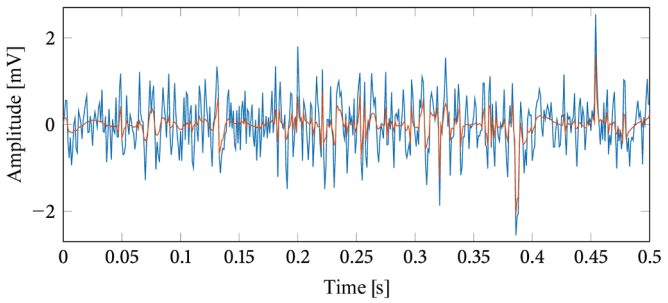

Fig. 11 SWT de-noised EMG signal (red) of former noisy EMG signal (blue) using bior1.3 wavelets, adaptive thresholding with WCF and threshold selection by minimax rule.

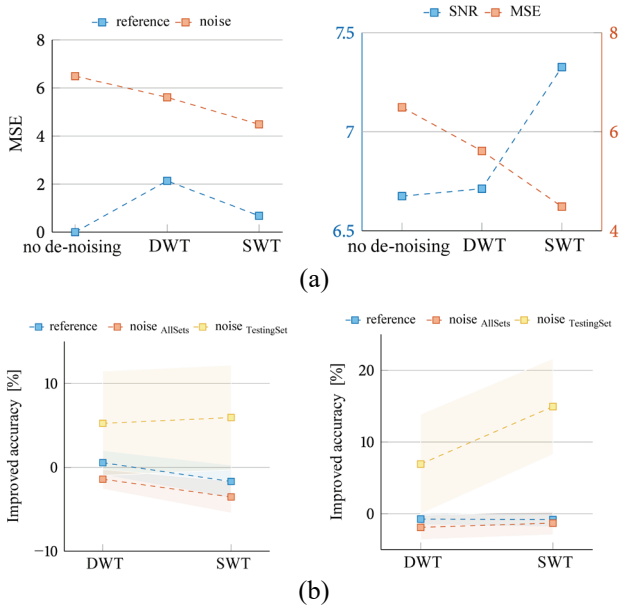

Fig. 10 Evaluation of SWT and DWT-based de-noising: (a) Error measures, (b) Changes in LDA-Acc (left) and MLP-Acc (right). Shaded error bars represent SD of the averaged EMG recording sessions (n=10).

D. *Wavelet-based Artifact Reduction – Offline*

Fig. 11 illustrates the artifact reduction performance comparing high-pass filtering with corner frequencies of 10, 20, 70 and 100 Hz, and our proposed wavelet algorithm. The wavelet algorithm outperformed conventional high-pass filtering in both SNR and MSE (see Fig. 11a). Mean segment-

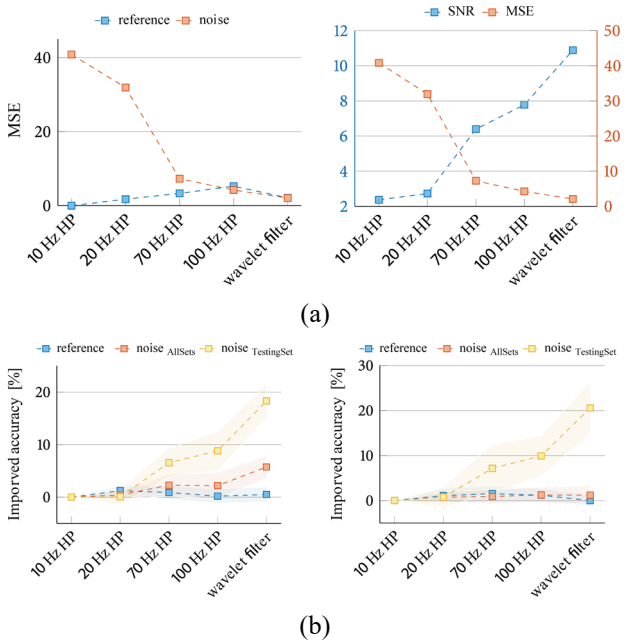

Fig. 9 Wavelet algorithm compared with conventional high-pass filtering: (a) Error measures, (b) Changes in accuracy using LDA (left) and MLP (right). Shaded error bars represent SD of the averaged EMG recording sessions (n=10). Wavelet filtering showed a statistically significant improvement over 10 Hz, 20 Hz, and 70 Hz filtering ($p < .05$) in the $\text{Noise}_{\text{TestingSet}}$ condition.

wise processing time for the wavelet algorithm was under 10 ms, which was considered small enough for real-time application. Furthermore, conventional high-pass filtering, especially at 70 and 100 Hz, caused higher MSE values as its application lead to changes throughout the whole signal whereas the wavelet algorithm modifies only the parts of the signal which are considered to be corrupted by artifacts.

The improved performance on the error measures was accompanied by a substantial improvement in the $\text{Noise}_{\text{TestingSet}}$ condition for both LDA and MLP classification for all filter corner frequencies except 100 Hz ($p < .05$). This indicates that using the algorithm proposed here is beneficial for real-time prosthetic control (see Fig. 11b).

We found that MLP classifier dealt relatively well with occurring artifacts if they appear regularly throughout the signal, as no improvement could be observed with any of the signal filtering techniques in the $\text{Noise}_{\text{AllSets}}$ condition (see Fig. 11b).

E. *Wavelet-based Artifact Reduction – Real-time*

After finding our wavelet based algorithm outperformed conventional high-pass filtering offline, the next step was to assess its real-time performance. Results of the real-time motion tests are illustrated in Fig. 12.

A reduction in completion time ($p < .01$) and an increase in accuracy ($p < .01$) were found on trial specific means when the proposed wavelet algorithm was applied, demonstrating its feasibility to operate in real-time.

It follows from these results that the detection and removal of motion related artifacts via a wavelet coefficient based algorithm outperforms conventional high-pass filtering and can be used in real-time applications such as prosthetic control.

This article has been accepted for publication in a future issue of this journal, but has not been fully edited. Content may change prior to final publication. Citation information: DOI 10.1109/TNSRE.2017.2771273, IEEE Transactions on Neural Systems and Rehabilitation Engineering

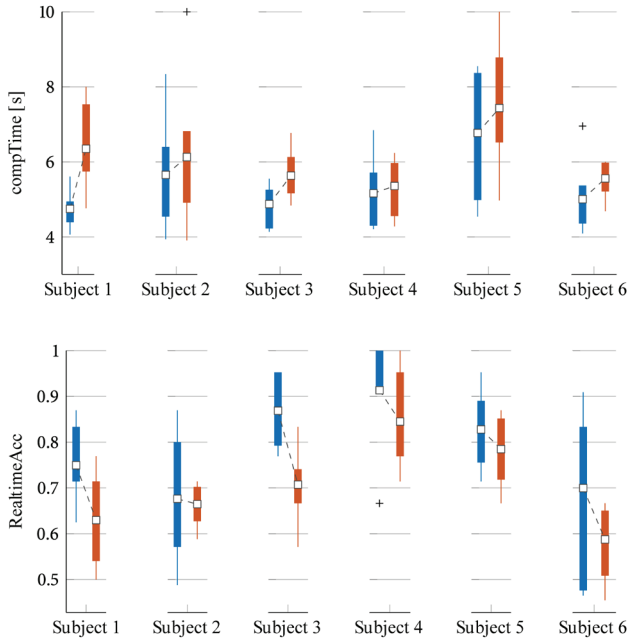

Fig. 12 Results of the real-time motion test. Blue bars show that the wavelet based algorithm was applied, whereas red bars illustrate the results for conventional high-pass filtering only.

V. Conclusion

Our results indicate that wavelet de-noising can be used to improve the robustness of EMG against changing noise without the pitfall of information losses when low or no noise is present.

We found that wavelet de-noising did not improve classification accuracies when high but consistent levels of noise were present. This is expected from machine learning algorithms that incorporate noise as part of the signal. In such ideal cases, improvement of SNR as a pre-processing step prior to classification is unnecessary. However, the ideal case is far from real-life usage.

We found that stationary wavelet transform (SWT) provided better results than discrete wavelet transform based de-noising. Although SWT has a higher computational cost, multi-signal processing can be applied in real-time, guaranteeing its usability in prosthetic control. Furthermore, the synthesis of Wavelet transform and Wiener filtering (Wavelet Wiener Filtering) provided promising results, and thus these should be further investigated since they have been scarcely discussed in the scientific literature.

In the second part of this work, we presented a wavelet-based algorithm which is capable of detecting and removing artifacts caused by rapid limb movements and mechanical interference. We found distinct advantages compared to conventional high-pass filtering, which is recommended in most literature. The algorithm proposed here outperformed conventional high-pass filtering with corner frequencies up to 100 Hz, and its feasibility in real-time processing was demonstrated.

The algorithms were implemented from a theoretical standpoint, and can be further optimized. Varying strategies of the algorithms proposed here regarding the definition of the threshold and the thresholding procedure will therefore be assessed in future work.

Acknowledgment

Author thanks to Enzo Mastinu for his support during this research, and to all the volunteers in this study.

References

[1] D. Farina und O. Aszmann, „Bionic limbs: clinical reality and academic promises," *Science translational medicine,* Bd. 6, Nr. 257, p. 257ps12, 2014.

[2] M. Carozza, G. Cappiello, G. Stellin, F. Zaccone, F. Vecchi, S. Micera und P. Dario, „On the development of a novel adaptive prosthetic hand with compliant joints: experimental platform and EMG control," in *Intelligent Robots and Systems, 2005.(IROS 2005). 2005 IEEE/RSJ International Conference on*, 2005.

[3] E. Biddiss und T. T. A Chau, „Upper limb prosthesis use and abandonment: a survey of the last 25 years," *Prosthetics and orthotics international,* Nr. 31, pp. 236--257, 2007.

[4] D. J. Atkins, D. C. Heard und W. H. Donovan, „Epidemiologic overview of individuals with upper-limb loss and their reported research priorities.," *JPO: Journal of Prosthetics and Orthotics,* Bd. 8, Nr. 1, pp. 2-11, 1996.

[5] N. Jiang, S. Dosen, K.-R. Müller und D. Farina, „Myoelectric control of artificial limbs: Is there a need to change focus," *IEEE Signal Process. Mag,* Bd. 29, Nr. 5, pp. 152-150, 2012.

[6] A. J. Young, L. J. Hargrove und T. A. Kuiken, „Improving myoelectric pattern recognition robustness to electrode shift by changing interelectrode distance and electrode configuration," *Biomedical Engineering, IEEE Transactions on,* Bd. 59, Nr. 3, pp. 645-652, 2012.

[7] A. Phinyomark, C. Limsakul und P. Phukpattaranont, „Wavelet-based denoising algorithm for robust EMG pattern recognition," *Fluctuation and Noise Letters,* Bd. 10, Nr. 2, pp. 157-167, 2011.

[8] N. Sobahi, „Denoising of EMG signals based on wavelet transform," *Asian Transactions on Engineering,* Bd. 1, Nr. 5, pp. 17-23, 2011.

[9] L. Citi, J. Carpaneto, P. Dario, K. Hoffmann, K. Koch, S. Micera und K. & Yoshida, „On the use of wavelet denoising and spike sorting techniques to process electroneurographic signals recorded using intraneural electrodes," *Journal of Neuroscience Methods,* Bd. 2, Nr. 172, pp. 294 - 302, 2008.

[10] L. J. Hargrove, G. Li, K. B. Englehart und B. S. Hudgins, „Principal components analysis preprocessing for improved classification accuracies in pattern-recognition-based myoelectric control," *Biomedical Engineering, IEEE Transactions on,* Bd. 56, Nr. 5, pp. 1407-1414, 2009.

[11] G. R. Naik, „A comparison of ICA algorithms in surface EMG signal processing," *International Journal of Biomedical Engineering and Technology,* Bd. 6, Nr. 4, pp. 363-374, 2011.

[12] L. Liu, P. Liu, E. A. Clancy, E. Scheme und K. B. Englehart, „Electromyogram whitening for improved classification accuracy in upper limb prosthesis control," *Neural Systems and Rehabilitation Engineering, IEEE Transactions on,* Bd. 21, Nr. 5, pp. 767-774, 2013.

[13] M. A. a. H. Amindavar, „EMG signal denoising via Bayesian wavelet shrinkage based on GARCH modeling," in *2009 IEEE International Conference on Acoustics, Speech and Signal Processing*, Taiwan, 2009.

[14] G. Aschero und P. Gizdulich, „Denoising of surface EMG with a modified Wiener filtering approach," *Journal of Electromyography and Kinesiology,* Bd. 20, Nr. 2, pp. 366-373, 2010.

[15] J. Liu, D. Ying und P. Zhou, „Wiener filtering of surface EMG with a priori SNR estimation toward myoelectric control for neurological injury patients," *Medical engineering & physics,* Bd. 36, Nr. 12, pp. 1711-1715, 2014.

[16] L. Sörnmo und P. Laguna, Bioelectrical signal processing in cardiac and neurological applications, Bd. 8, Academic Press, 2005.

[17] S. Mallat, A wavelet tour of signal processing, Academic press, 1999.

[18] G. P. Nason und B. W. Silverman, The stationary wavelet transform and some statistical applications, 281-299 Hrsg., New York: Springer, 1995.

[19] S. P. Ghael, A. M. Sayeed und R. G. Baraniuk, „Improved wavelet denoising via empirical Wiener filtering," in *Optical Science, Engineering and Instrumentation*, 1997.

[20] L. Smital, M. Vitek, J. Kozumplik und I. Provaznik, „Adaptive wavelet wiener filtering of ECG signals," *Biomedical Engineering, IEEE Transactions on,* Bd. 60, Nr. 2, pp. 437-445, 2013.

[21] BioPatRec, „Wiki," [Online].
Available: https://github.com/biopatrec/biopatrec/wiki.

[22] E. Mastinu, M. Ortiz-Catalan und B. Hakansson, „Analog Front-Ends comparison in the way of a portable, low-power and low-cost EMG controller based on pattern recognition EMBC 2015," in *Engineering in Medicine and Biology Society (EMBC), 2015 37th Annual International Conference of the IEEE*, 2015.

[23] I. Nabney, NETLAB: algorithms for pattern recognition, Springer Science & Business Media, 2002.

[24] M. Ortiz-Catalan, R. Brånemark und B. Håkansson, „BioPatRec: A modular research platform for the control of artificial limbs based on pattern recognition algorithms," *Source code for biology and medicine,* Bd. 8, Nr. 1, p. 1, 2013.

[25] M.-F. Lucas, A. Gaufriau, S. Pascual, C. Doncarli und D. Farina, „Multi-channel surface EMG classification using support vector machines and signal-based wavelet optimization," *Biomedical Signal Processing and Control,* Bd. 3, Nr. 2, pp. 169-174, 2008.

[26] T. A. Kuiken, G. Li, B. A. Lock, R. D. Lipschutz, L. A. Miller, K. A. Stubblefield und K. B. Englehart, „Targeted muscle reinnervation for real-time myoelectric control of multifunction artificial arms," *Jama,* Bd. 301, Nr. 6, pp. 619-628, 2009.

Julian Maier was born in Karlsruhe, Germany in 1988. He graduated with the final federal medical exam in 2013 and received the academic degree Doctor of Medicine (Dr. med.) from the University of Heidelberg, Germany, in 2014. He received the M.Sc. degree in biomedical engineering from the University of Stuttgart, Germany, in 2016.

Adam Naber was born in California, U.S.A. in 1988. He graduated from California State University, Sacramento, U.S.A., with a B.S. degree in computer engineering in 2013. He obtained the M.Sc. degree in biomedical engineering from the Chalmers University of Technology, Gothenburg, Sweden, in 2017. He is currently pursuing his Ph.D. at the Biomechatronics and Neurorehabilitation Laboratory (@ChalmersBNL) at Chalmers University of Technology.

Max Ortiz Catalan (M'14) was born in Toluca, Mexico in 1982. He received the Electronic Engineering degree in 2005 from the ITESM Campus Toluca, Mexico, the M.Sc. degree in complex adaptive systems in 2009, and the Ph.D. degree in biomedical engineering in 2014 from Chalmers University of Technology (CTH), Gothenburg, Sweden. He is currently an Associate Professor at CTH, where he founded the Biomechatronics and Neurorehabilitation Laboratory (@ChalmersBNL). He also serves as Research Director for Integrum AB, Sweden. He received the "European Youth Award" in 2014, the "Delsys Prize" in 2016, and the "Brian & Joyce Blatchford Award" in 2017.